JOM
DOI: 10.1007/s11837-015-1569-3
© 2015 The Minerals, Metals & Materials Society

Thermal and Morphological Study of Epoxy Matrix with Chemical and Physical Hybrid of Nanoclay/Carbon Nanotube

ELNAZ ESMIZADEH,[1] GHASEM NADERI,[1,3] ALI AKBAR YOUSEFI,[1] and CANDIDA MILONE[2]

1.—Faculty of Polymer Processing, Iran Polymer and Petrochemical Institute (IPPI), P.O. Box 14965/115, Tehran, Iran. 2.—Dipartimento di Ingegneria Elettronica, Chimica e Ingegneria Industriale, Università di Messina, 98166 Messina, Italy. 3.—e-mail: G.Naderi@ippi.ac.ir

Synergistic effects of nanoclay (NC) and carbon nanotube (CNT) as a physical and chemical hybrid on the properties of epoxy matrix were studied. The chemical hybrid of CNT-NC (CNC) was synthesized by high-temperature decomposition of methane on NC supports. The formation of CNTs on the NC surface was confirmed by transmission electron microscopy, scanning electron microscopy (SEM) and Raman spectroscopy. As-prepared CNCs were subsequently added into an epoxy matrix to make epoxy-CNC composites. The mixture of purified CNTs and NC as the physical hybrid of CNT-NC (PNC) was introduced into the epoxy matrix in order to fabricate epoxy-PNC composites. The relationship between the type of filler with the thermal and morphological performance of the epoxy-CNT-NC composite hybrids was investigated. The exfoliation characteristics of NCs and CNTs in epoxy nanocomposites were analyzed using x-ray spectroscopy (EDX) and SEM studies, respectively. Thermal behavior of the epoxy nanocomposites was studied by thermo-gravimetric-differential thermal analysis (TGA/DTG), the heat deflection temperature (HDT) test and dynamic mechanical analysis (DMA). The results indicated that the thermal characteristics of the epoxy including the degradation temperature (T_{deg}), HDT and glass transition temperature (T_g) relatively increased with the introduction of all the nanofillers, NC, CNT, PNC and CNC. The synergistic effects of CNT and NC were found to be more marked for the chemical hybrid compared to the physical one. In the case of CNC, it was observed that the CNTs attached to the clay sheets form a unique structure in which a 2D NC has several 1D CNTs attached to it. The enhanced homogeneous dispersion of NCs and CNTs in epoxy-CNC was clearly observed compared to epoxy-PNC.

INTRODUCTION

In recent years, much attention has been paid to the preparation of high-performance polymer nanocomposites using a combination of nanofillers with different dimensions. Carbon nanotubes (CNTs) as 1D nanomaterials have been considered to be ideal reinforcing fillers for a polymer matrix because of their unique structural,[1] electrical, mechanical, electromechanical and chemical properties.[2] On the other hand, clay platelets as 2D nanomaterials have the potential of being low-cost alternative fillers for incorporation into polymeric matrices for commercial applications.[3] Thus, the concurrent application of CNTs and nanoclay (NC), as both the physical and chemical hybrid filler in polymers has provided the advantages of both fillers to improve the properties.

Incorporation of NC was proposed as an effective method for dispersion of CNTs into the thermosetting epoxy matrix.[4,5] Sun et al. reported the improved dispersion of CNTs in the presence of NC benefiting from the strong electrostatic affinity between these two nanofillers.[4] Liu et al. showed that the CNT morphology of epoxy-CNT nanocomposites changed from discontinuous aggregated clusters to a continuous three-dimensional network by the addition of NC.[5] Tarawneh et al. discussed

Published online: 07 August 2015

the processing of natural rubber/physical hybrids of CNT and NC nanocomposites with different percentages of filler in order to obtain the optimum mechanical and thermal properties.[6,7] A polypropylene (PP) nanocomposite system with improved flame retardancy and thermal stability was obtained utilizing the unique properties of NC in combination with CNTs.[8–10] The mechanism proposed for improved thermal stability involved the physical/chemical adsorption of volatile degradation products on the nanofiller surface.[9,11] Furthermore, a high degree of exfoliation accompanied by fine dispersion was required to increase the overall thermal stability of the polymer matrix.[11] Apart from improvement in thermal stability, the increase in elastic modulus, loss modulus and glass transition temperature (T_g) of polymers was observed with the simultaneous addition of NC and CNTs.[5] In the case of wood–polymer composites, the synergistic effect of NC and CNTs enhanced the interaction between wood and polymer leading to a restriction in polymeric chain movement and higher T_g.[12]

Although the advantages of using physical hybrids of CNTs and NC are well documented in the literature, the application of chemical hybrids of them is still a novel and challenging task. Iron, nickel, or cobalt nanoparticles supported on NC were efficient catalysts for the synthesis of CNTs on NC surfaces by chemical vapor deposition (CVD). This method has been proved to be a cost-efficient and facile approach to fabricate chemical hybrids of CNTs and NC.[13] These hybrids have been shown to be promising nanofillers to improve the properties of a polymer.[14,15]

Recently, the synergistic effect between CNTs and NC in chemical hybrids of them was evidenced with outstandingly enhanced mechanical properties of polymer nanocomposites with respect to the pristine polymer.[16–18] Strong interaction between the chemical hybrid and the polymer was proved to be responsible for that significant improvement.[13] Improvement in thermal stability was observed for polyurethane foams,[18] nylon-6[19] and Nafion[20] with chemical hybrids of CNTs and NC. The considerable improvement was related to the possible mechanical interlocking which may occurred within the polymer matrix owing to the structure of the hybrids, which facilitates the exfoliation of the clay in the matrix.[16]

As mentioned, synergistic effects of NC and CNTs as physical and chemical hybrids on the properties of a polymer matrix have been recently reported.[16,18,20] However, systematic studies about the comparative effect of the simultaneous use of NCs and CNTs as chemical and physical hybrids on the properties of polymer matrixes have not yet been reported. Hence, there is a lot of scope to do further work in this area. In this study, the growth of CNTs through methane CVD on clay-supported iron nanoparticles as a catalyst applied to prepare a chemical hybrid of CNT-NC (CNC). The process was followed by the incorporation of as-prepared CNCs into an epoxy matrix to make epoxy-CNC composites. A physical mixture of CNTs and NC as a physical hybrid of CNT-NC (PNC) was introduced into an epoxy matrix in order to fabricate epoxy-PNC composites. The main objective of this work is to study the synergistic effect of CNT-NC hybrids (both chemical and physical) on the thermal behavior of the composites by dynamic mechanical analysis (DMA), heat deflection temperature (HDT) and thermo-gravimetric-differential thermal analysis (TGA/DTG). The correlation between thermal performance and the morphology of the filler in the epoxy matrix filled with CNT-NC hybrids was investigated.

EXPERIMENTAL

Materials

CVD experiments were carried out on an organo-modified montmorillonite (MMT), Cloisite® 15A, produced by Southern Clay Products (USA) as the support. Iron (III) nitrate nonahydrate [>99%, Fe $(NO_3)_3{\cdot}9H_2O$; Merck-Germany)], methane (99.99%), hydrogen (99.99%) and nitrogen (99.99%) (Roham Gas, Iran) were used as received. The polymer matrix (Araldite LY 5052/Aradur HY 5052; Huntsman, Switzerland) was used as a standard low viscosity epoxy[3] along with a hardener based on modified cycloaliphatic amines (HY5052).

Methods and Characterizations

Preparation of NC-Supported Fe Catalysts

NC-supported Fe catalysts were prepared according to the Ref. [13] by the wet-impregnation method. In a typical procedure, a NC solution (10 g in 150 mL of deionized water) was stirred with iron (III) nitrate solution (18 g in 100 mL of deionized water) overnight at room temperature. After stirring, the solvent was evaporated at 100°C on a hot plate. The resulting paste was dried under vacuum for 8 h and calcined at 500°C for 3 h. The obtained brown solid was ground into fine powder, screened by a 100-mesh sieve and then reduced for 2 h under (60 mL/min) hydrogen flow at 500°C.

CVD Growth of CNTs

CNTs were grown on the Fe-immobilized NC by catalytic CVD with methane at 950°C.[21] For CNT growth, a quartz boat containing the catalyst powder was placed in a quartz tube kept in a horizontal tube furnace model P. Tube 12/38/750 (Pyro Therm Furnaces, Leicester, UK). The furnace was heated to 950°C under a nitrogen stream to remove any trace of moisture and oxygen present in the reactor.[22] Thereafter, the CNTs were grown under the flow of the reactant gases over the catalyst for 1 h. After the completion of CNT growth the furnace was

cooled to room temperature under a nitrogen stream. Finally, the quartz boat was taken out of the furnace and the reaction product was represented here as CNC.

Purification of As-grown CNTs

In order to compare the effect of the chemical and physical CNT-NC hybrids more reliably, as-grown CNTs were purified and then used in PNC. For this purpose, the NC support and iron particles were removed by refluxing the obtained CNC in a mixture of 12% HCl and 12% HF acids, respectively.[23] Finally, the CNT deposits were washed thoroughly with distilled water and dried overnight at 80°C.

Preparation of Epoxy Nanocomposites Based on Hybrid of CNT-NC

The epoxy nanocomposites were prepared using a mixing and casting method, which included the following steps:

(a) Adding the pre-determined mass fractions of nanofiller to the hardener and mixing for 30 min with ultra-sonication (60% Ampl) in an ice bath
(b) Adding the epoxy and mixing by a mechanical shaft in an ice bath (900 rpm) for 5 min to ensure good homogeneity
(c) 1 h of degassing by vacuum at room temperature
(d) Casting the mixture in silicone molds
(e) 24 h cure at room temperature
(f) 4 h post-cure at 100°C

The mass ratio of epoxy/hardener (Araldite LY 5052/Aradur HY 5052) was kept 100:38 according to the manufacture's data-sheet.[24]

Characterization

The surface area of the support was measured using the Brunauer–Emmett–Teller (BET) method at every stage of the catalyst preparation by a single-point BET surface analyzer (Quantachrome TPR Win v.1.0; USA) using nitrogen as the adsorbate. Small- and wide-angle x-ray scattering (SAXS and WAXS) patterns were collected by a Philips X'Pert MPD (Netherlands) diffractometer using a CuKα radiation source at 40 kV and 40 mA with step size of 0.02°/s. The basal spacing (d_{001}) was measured using Bragg's equation.[25] Raman spectra were recorded by a Micro-Raman system, RM 1000 RENISHAW, using a 50-mW laser excitation line at 785 nm equipped with a Leica DMLM microscope and a Peltier-cooled charge-coupled device (CCD) detector. Surface morphology and the overall quality of the CNT dispersion in the epoxy matrix were investigated by a VEGA/TESCAN (Czech Republic) scanning electron microscope (SEM). Energy-dispersive x-ray (EDX) spectroscopy coupled with SEM was used to verify the validity of the location of the NC particles. As a priori to study the fracture surface, the SEM specimens were prepared by fracturing the samples in liquid nitrogen. The samples were gold-sputtered to reduce the electrostatic charge generated by the electron beam bombardment. Transmission electron microscopy (TEM) was performed on a Philips EM 208 (Germany) under an accelerated voltage of 100 kV. The heat distortion temperature (HDT) (Ats Faar, Italy) of the nanocomposites was measured under load (1.8 MPa) according to ASTM D 648. Dynamic mechanical properties of epoxy nanocomposites were measured using DMA-TRITON (TRITEC 2000 DMA; Lincolnshire, UK) according to ASTM-E 1640-04. Temperature scans were carried out with a frequency of 1 Hz at a heating rate of 5°C/min in the temperature range of 25–180°C. TGA/DTG analysis was carried out on a Perkin–Elmer Pyris instrument (USA) heating from room temperature to 1000°C under the ambient atmosphere, using a ramp rate of 10°C/min.

RESULTS AND DISCUSSION

Structural Properties of the Catalysts

The specific surface area (S_{BET}) and total specific pore volume of NC support in the catalyst preparation stages are reported in Table I. After wet impregnation, no considerable change in the surface area was observed, compared to the pristine NC. The calcination of the impregnated support caused a drastic increase in the S_{BET} value. This showed that the calcination process greatly expanded the active surface areas of the support.[26] After calcination, the metallic cations were transformed to oligo-nuclear metal oxides, strongly immobilized on the clay surfaces.[27]

Figure 1a presents the WAXS pattern of the NC on different stages of the catalyst preparation. Several 2θ peaks were observed in the diffractogram of pristine Cloisite® 15A (Fig. 1a-i) indicating the layered structure of montmorillonite. The peaks located at 20°, 35°, 54°, and 62° were attributed to the diffraction of (110), (105), (210), and (300) reflections of the montmorillonite, respectively.[23,28] The sample obtained after calcination (Fig. 1a-ii) still showed the peaks indicative of montmorillonite structure. The other diffraction peaks in this sample had been indexed with Fe_2O_3.[29] This showed that, during the calcination process, Fe^{3+} ions, which intercalated into the layers of montmorillonite by wet impregnation with the Fe $(NO_3)_3$ solution, changed to Fe_2O_3.[13] The reduced support gave the most intense diffraction peak at 44.7° (Fig. 1a-iii), in addition to the pristine support peaks. This diffraction peak was well matched with that for the metallic Fe,[29] indicating that, during the reduction process, Fe_2O_3 particles reduced to the metallic state. The literature[13,23] also states that Fe_2O_3 should convert to metallic Fe to serve as seeds for the growth of CNTs under CVD, which was consistent with the WAXS pattern observed in this work.

Table I. Specific surface area (S_{BET}) of NC support in catalyst preparation stages

Samples	Pristine support	Impregnated support	Calcinated support	Reduced support
Specific surface area (m^2/g)	4.86	5.14	65.60	54.87
Total specific pore volume (mL/g)	0.0026	0.0028	0.0357	0.0298

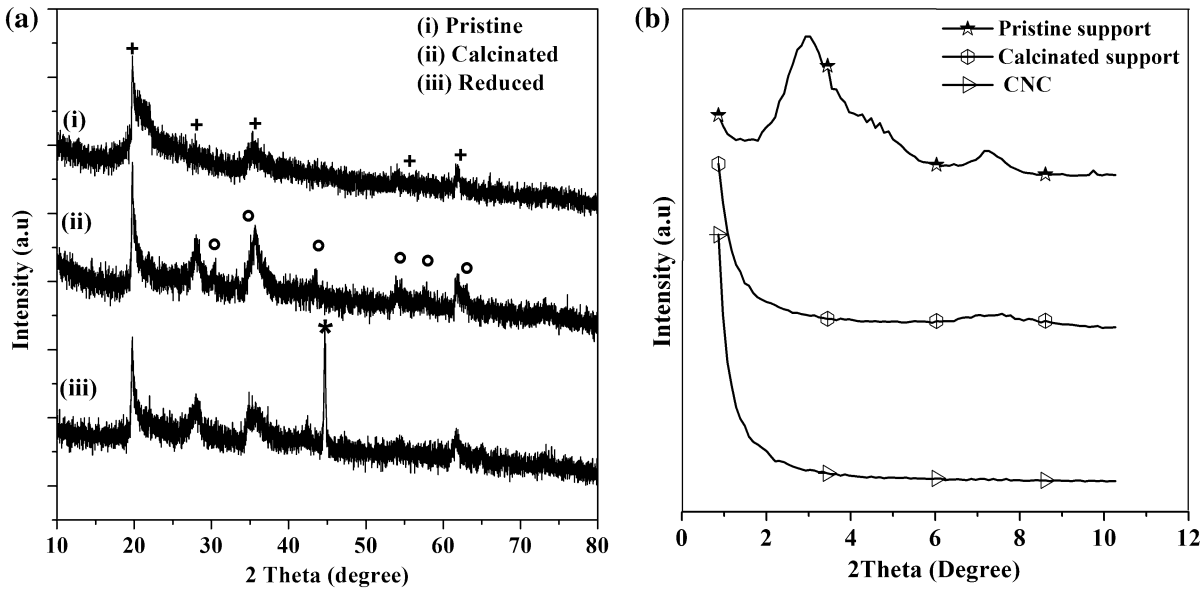

Fig. 1. (a) WAXS spectra of *i* Pristine support (Cloisite ®15A), *ii* calcinated Fe-loaded support, and *iii* reduced Fe-loaded support. (+) Montmorillonite, (o) oxidized Fe-Fe_2O_3, (*) metallic Fe. (b) SAXS spectra of pristine support, calcinated Fe-loaded support and CNC.

The SAXS patterns of pristine support, the calcinated one and NC after CVD (CNC) shown in Fig. 1b, reveal that calcination of the Fe-loaded OC (Cloisite®15A) and further CVD reaction has a severe effect on its [001] reflection. The disappearance of basal reflection at $2\theta = 2.8°$ corresponded to 001-$d_{spacing}$ in XRD patterns of the calcinated support with respect to the parent NC suggested the strong delamination of the structure. The delamination could be caused by the degradation of quaternary ammonium salt modifiers during calcinations.[30] Then, the layers of the NC were further delaminated in CNC due to the growth of CNTs on the platelets, as previously observed.[13]

Chemical Hybrid of CNT-NC (CNC)

The morphology and dimensions of the carbonaceous products grown by CVD (CNC) were investigated by SEM and TEM (Fig. 2). SEM analysis of as-grown carbonaceous products on the catalyst (Fig. 2a and b) evidenced that filamentous structures were successfully produced over the Fe-loaded clay as the catalyst, in agreement with our results previously obtained on Na^+-exchanged clay.[31] The filamentous structure (which will be proven to be CNTs below) were highly entangled in bundles which might indicate the presence of defects in the CNTs structure.[31]

TEM observation was conducted to obtain more details about the morphology of the CNC, as shown in Fig. 2c. The clearly hollow nature of the as-grown carbonaceous products on NC revealed the successful formation of multi-walled carbon nanotubes (MWCNTs). Encapsulated Fe-nanoparticles (with diameters greater than 5 nm) within the channels of the nanotubes showed the crucial role of Fe_3C in CNT growth by the CVD method.[32] Furthermore, it can be seen that the CNTs are randomly distributed and attached to the NC sheets. This revealed the formation of a unique 3D structure in which a 2D clay platelet has several 1D nanotubes attached to it. The SEM image of the separated CNTs from CNC was obtained after purification process (Fig. 2d, which indicates that the CNTs structure still prevails even after purification. Dimension measurements of Fig. 2b showed that the outer diameter of the CNTs ranges from 15 nm to 150 nm and the length is between 4 μm and 25 μm. The distribution of the as-grown CNTs' length and diameter obtained from several SEM micrographs (not shown here) is illustrated in Fig. 3.

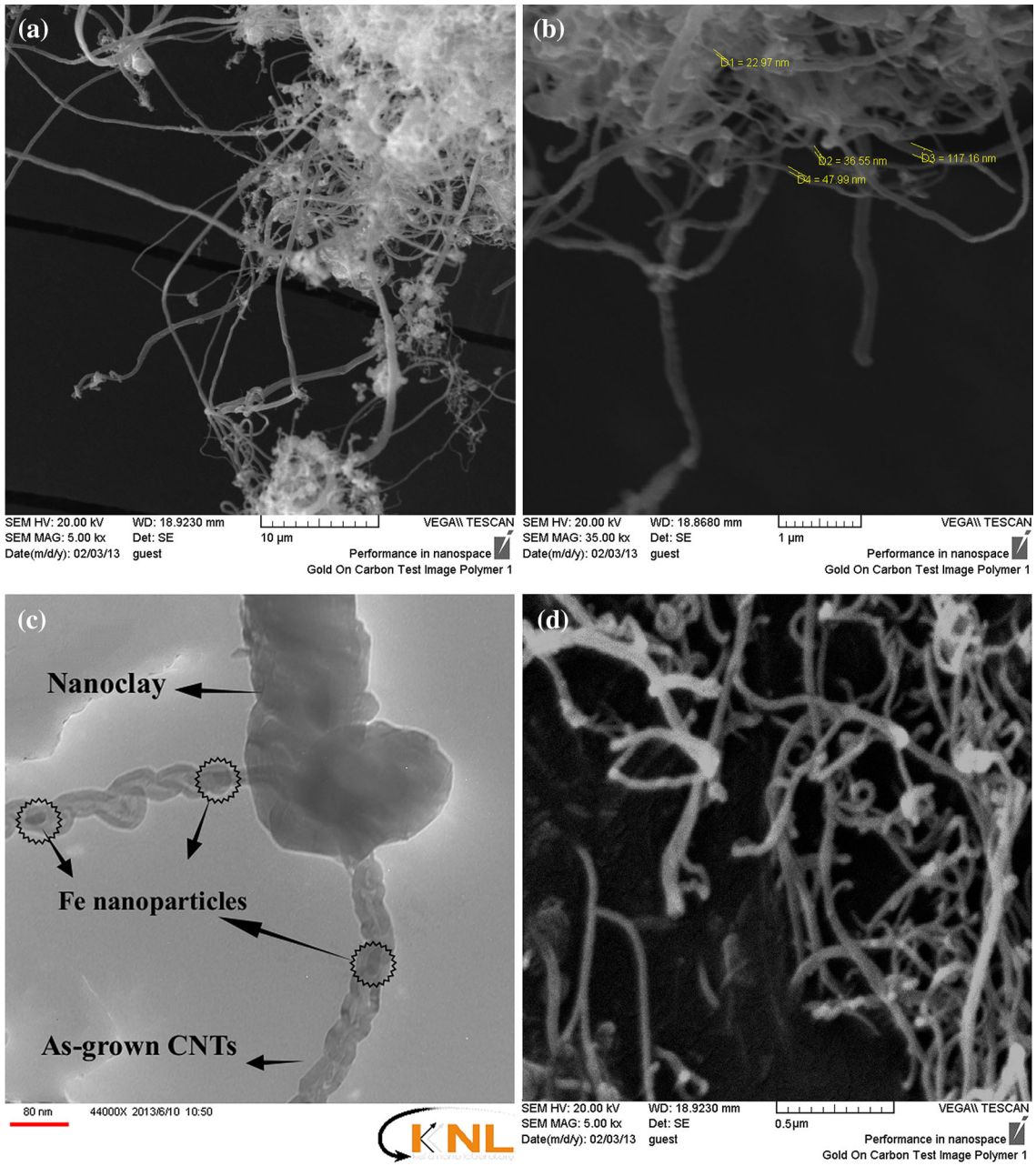

Fig. 2. Morphology of CNTs obtained by methane CVD over Fe-loaded NC: (a, b) SEM and (c) TEM of product before purification (CNC), (d) SEM of purified CNTs.

Raman spectroscopy was used to characterize as-prepared CNC sample and also provide information on the nature of the as-grown CNTs on NC. Figure 4 displays the shape evolution of the Raman spectra. In the Raman spectrum of a typical MWCNT, three modes were often observed at 1340–1350 cm^{-1}, 1570–1610 cm^{-1} and 2700–2800 cm^{-1}, referred to as the D-, G- and G′-bands, respectively. The D peak was related to the presence of lattice disorder and defects in the sidewall structure of the CNTs. The G peak was associated with the in-plane vibrations of the graphene sheet related to the crystalline graphitic carbons. The overtone of the D-band, the so-called G′-band, was defect-independent.[31]

The relative intensity of the D and G bands (I_D/I_G) indicates the degree of disorder in the graphite sheets. The I_D/I_G ratio can be used as a measure of the crystallinity of the synthesized CNTs and it was found to be 1.4. The average size of domains with graphitic order ($L_C = 560 \cdot (I_G/I_D) \cdot E_L^{-4}$)[33] was calculated to be 62.0 nm, where E_L was the laser visible excitation energy (1.58 eV in our case). These values were

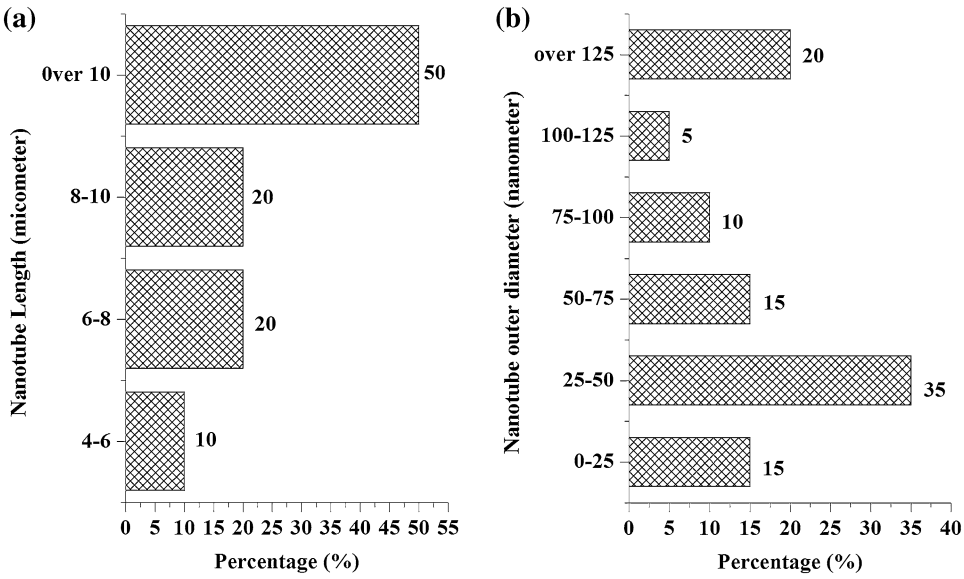

Fig. 3. Percent dimension distribution of as-grown CNTs present in CNC: (a) length and (b) diameter.

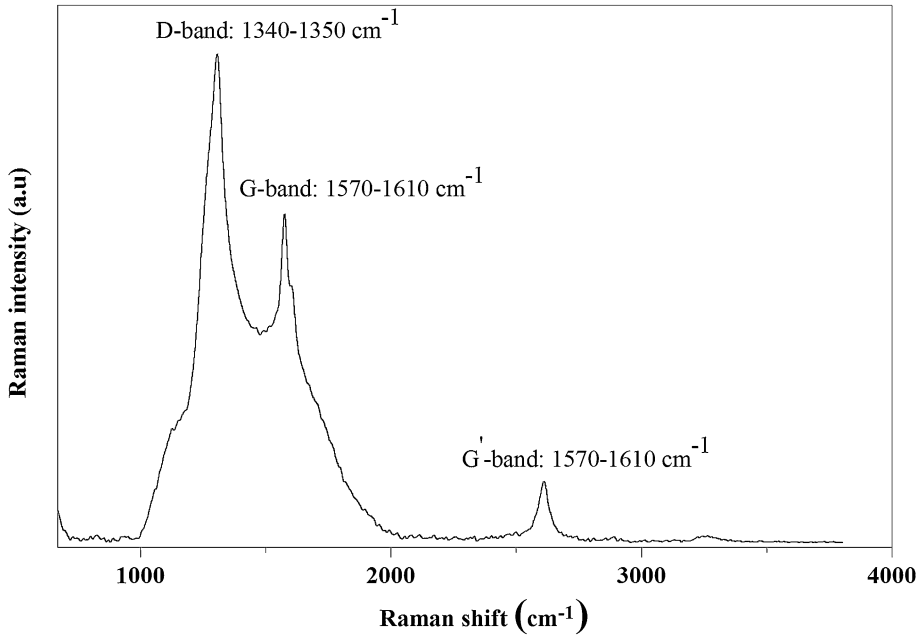

Fig. 4. Shape evolution of Raman spectra of as-grown CNTs present in CNC.

similar to those reported in the literature for CNTs prepared using CVD on NC support, revealing the acceptable quality of the prepared CNTs.[34,35] The relative intensity of the D-band to the G-band ($I_D/I_G > 1$) revealed that the MWCNTs were grown on our catalyst rather than single-walled CNTs (SWCNTs). Due to the fact that SWCNTs typically show a stronger intensity of the G-band compared to that of the D-band.[21] Predominant growth of MWCNTs was expected because the synthesized nanotubes originated from Fe nanoparticles with diameters higher than 5 nm (as shown in Fig. 2c.

Even though the Raman spectrum verified the formation of MWCNTs, TGA was used for further confirmation according to the combustion temperature of MWCNTs. TGA and DTG results of the CNC before and after purification, in an atmosphere of oxygen, are shown in Fig. 5. No significant weight loss below 400°C was evidenced by the TGA measurements, indicating little/no amount of amorphous carbon was present in the synthesized CNTs. The peaks typically occurring over 400°C can be utilized to estimate the type of carbonaceous structures.[27]

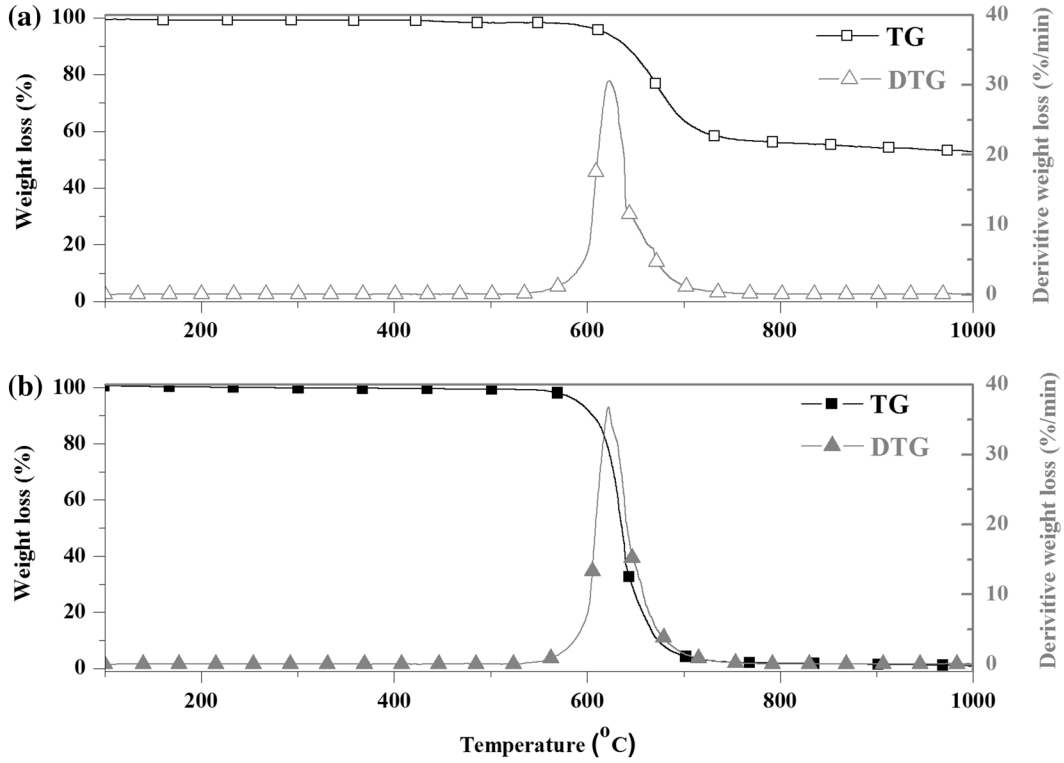

Fig. 5. Thermal stability of (a) CNC and (b) CNTs obtained after purification of CNC; as monitored by TGA/DTG curves.

Table II. Mass content and type of nanofiller used in preparation of epoxy nanocomposites

		Nanofiller	
Sample no	**Sample code**	**Content (%) by mass**	**Type**
1	Epoxy	0	–
2	Epoxy-0.2 NC	0.2	Nanoclay support just before CVD reaction
3	Epoxy-0.2 CNT	0.2	Carbon nanotubes after purification of CNC
4	Epoxy-0.2 PNC	0.2	Mixture of NC[a] and CNT[b] (50/50)
5	Epoxy-0.2 CNC	0.2	CNC

[a]Nanoclay support just before CVD reaction[b]Carbon nanotubes after purification of CNC.

The TGA curves of CNC both before and after purification present a single mass drop at ~619°C with mass losses of ~50% and 100%, respectively. The residual mass, above 700°C (Fig. 5b), was mainly attributed to the NC remaining in the sample.[36] The maximum exothermic peak (T_{peak}) of DTG curve which was located at 619°C can be attributed to the combustion of the MWCNTs. The high resistance to oxidation (above 600°C) of the carbon nanostructures grown over the NC catalyst revealed that they were MWCNTs. According to the literature, SWCNTs typically show less thermal stability (below 600°C) than MWCNTs due to the strong interaction between graphene layers in the MWCNTs.[37] By subtracting the value of the mass drop at ~619°C, the yield of MWCNTs in the synthesized CNC was estimated to be ~50% (Fig. 5a). Figure 5b shows the TGA/DTG results of the CNC after purification. During purification, the MWCNTs underwent acid wash to remove the NC and catalyst particles. Since the DTG peak was almost unchanged, it can be concluded that purification caused little or no damage to the structures of the synthesized MWCNTs. The purified MWCNTs were further used in preparation of PNC in the following experiments.

Epoxy Nanocomposites Based on Hybrids of CNT-NC

In an effort to compare the effect of CNC on properties of epoxy with PNC, NC and CNT, the epoxy nanocomposite samples were prepared according to Table II. Samples were identified as

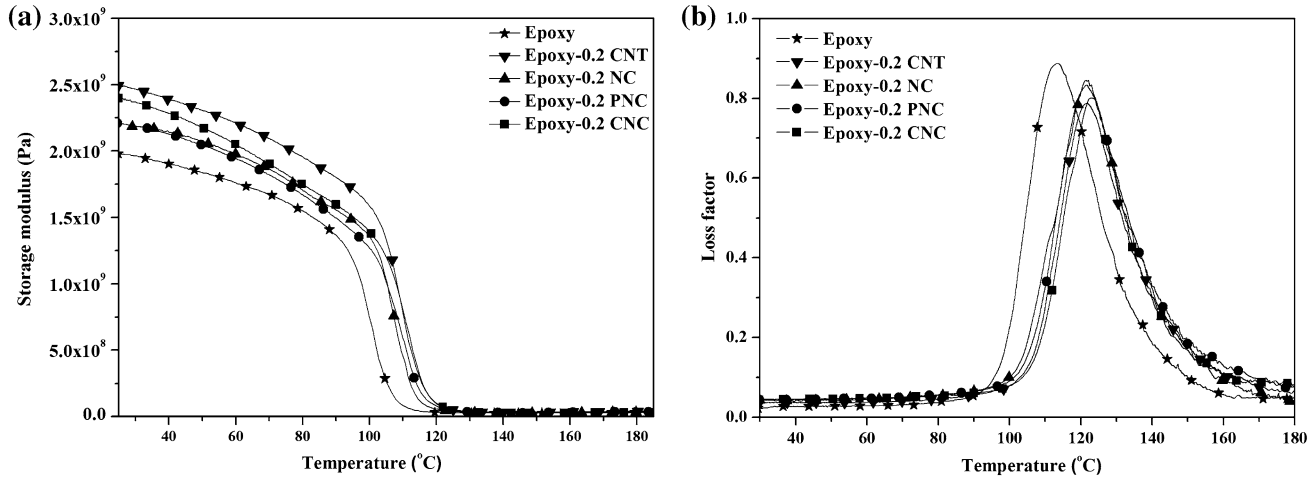

Fig. 6. (a) Storage modulus (E′) and (b) loss factor (tan δ) versus the temperature curves for epoxy nanocomposites.

Table III. DMA, TGA/DTA results of epoxy and its nanocomposites containing different nanofillers

	DMA		TGA/DTA		
Sample code	**Storage modulus (GPa) at 25°C**	**Glass transition temperature (°C)**	T_{on} (°C)	T_{deg} (°C)	**Residual mass (%)**
Epoxy	1.97	113	340.1	369	10
Epoxy-0.2 NC	2.21	121	342.6	372	11
Epoxy-0.2 CNT	2.51	121	341.3	370	11
Epoxy-0.2 PNC	2.21	121	342.9	374	12
Epoxy-0.2 CNC	2.38	123	344.3	375	13

"Epoxy" followed by the mass percentage and the type of the nanofiller, respectively. For example, the sample containing 0.2% mass content of CNC was identified as Epoxy-0.2 CNC.

Figure 6 illustrates the effect of different nanofillers on the storage modulus (E') and loss factor (tan δ) of the prepared epoxy nanocomposites. At low temperature (glassy regime), the introduction of 0.2 wt.% nanofiller caused a remarkable increase in the storage modulus compared to neat epoxy (Fig. 6a). The improvement of the storage modulus, with the introduction of nanoparticles was the result of the extraordinary stiffness of CNTs, NCs and their hybrid. The samples with 0.2 wt.% CNT and 0.2 wt.% NC show 28% and 12% increases in storage modulus compared to neat epoxy, respectively (Table III). The higher reinforcing effect of CNTs compared to NC due to their higher modulus was also observed in our previous work.[38] The samples with 0.2 wt.% PNC and 0.2 wt. CNC showed 12% and 20% higher storage modulus than the neat epoxy, respectively. This result provided the evidence that the CNC could be more effective in enhancing the storage modulus of epoxy compared to PNC. Not much difference in the E' was seen for epoxy nanocomposites in a high temperature or rubbery regime.

The maximum of the tan δ curve (peak temperature) was considered as the glass transition temperature (T_g) of the composite. Figure 6b reveals that all epoxy nanocomposites show slightly higher T_g than unfilled epoxy. Nanocomposites with 0.2 wt.% CNT, NC and PNC had a quite similar T_g value, 121°C, while the addition of 0.2 wt.% CNC increased it from 113°C, when there was no nanofiller, to 123°C (Table III). This could be an indication that high interactions between polymeric chains and filler made the movement of the polymer chains more restricted.[19] In addition, the net structures of CNT and NC and their hybrids might effectively restrict the movement space and mobility of the epoxy chains.[14]

In order to develop an understanding of the interactions of nanofillers with the epoxy matrix, fractography of the fracture surface of the epoxy nanocomposites was performed by SEM. Figure 7a–e displays the fracture surface of the epoxy with different types of nanofiller. As can be observed in Fig. 7a, the fracture surface of the virgin epoxy was very smooth but there was a significant increase in average roughness with the introduction of nanofiller. The higher roughness of the fracture surface of epoxy-0.2 CNC compared to epoxy-0.2 PNC confirmed the higher interaction between the epoxy matrix and the CNC. This observation is in good agreement with the T_g results of the DMA analysis.

The homogeneous dispersion of nanofillers in a polymer matrix is the key factor to obtain high-performance composites.[13] In order to support the

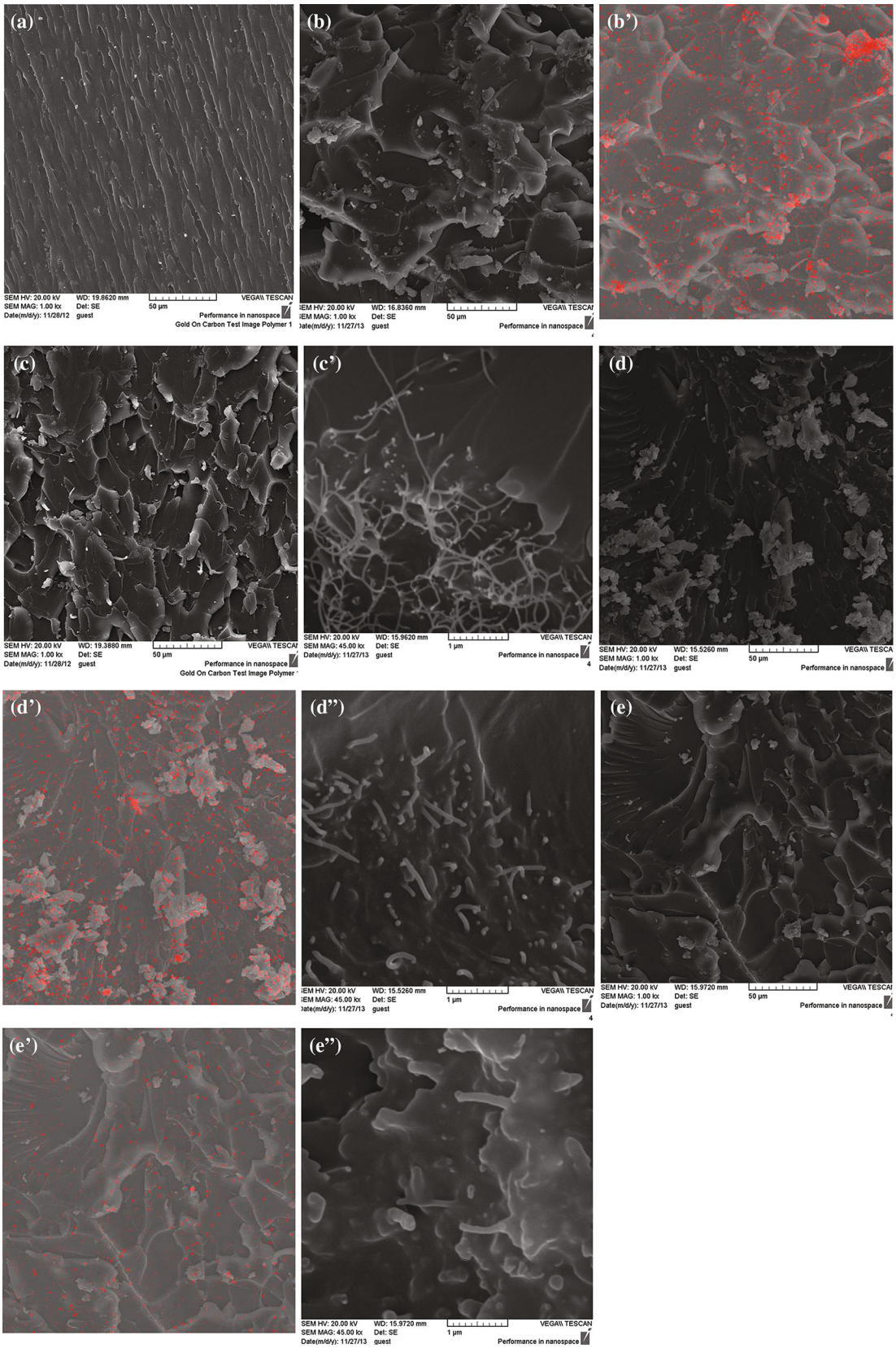

Fig. 7. Fracture surface of (a) epoxy, (b) epoxy-NC, (c) epoxy-CNT, (d) epoxy-PNC and (e) epoxy-CNC by SEM. Dispersion status of NC (b′): epoxy-NC, (d′) epoxy-PNC and (e′) epoxy-CNC with detection Si by EDX. Dispersion status of CNT: (c′) epoxy-CNT, (d″) epoxy-PNC and (e″) epoxy-CNC by high-magnification SEM.

good dispersion of nanofillers in the epoxy matrix, EDX and high-magnification SEM were applied to detect NC and CNT, respectively. The red points in Fig. 7b′ were related to the main element of NC, silicone (Si).[39] According to the photograph, epoxy-0.2 NC developed a homogenous dispersion, since very few silicate layers gathering in tactoids can be observed. Figure 7c′ shows the SEM image of the epoxy-0.2 CNT sample. It can be seen that the CNTs were randomly dispersed and no aggregation of CNTs is observable. Randomly dispersed CNTs in epoxy-0.2 PNC and epoxy-0.2 CNC nanocomposites are shown in Fig. 7d″ and e″, respectively. The observation that most CNTs were broken upon failure rather than just pulled out of the epoxy is an obvious confirmation of the strong interfacial adhesion between the nanofiller and the epoxy matrix.[13] In the case of epoxy-0.2 CNC, the unique 3D structure of the CNC, including the 2D NC with several 1D CNTs attached to it, can be seen in Fig. 7e″. The more homogeneous dispersion of the NC in the epoxy matrix was obvious from the EDX analysis of epoxy-0.2 CNC (Fig. 7e′) compared to that of epoxy-0.2 PNC (Fig. 7d′).

Variation in the HDT of the epoxy nanocomposites is illustrated in Fig. 8. It can be observed that, by the introduction of 0.2 wt.% of CNT and NC, the increase in the HDT of the epoxy was about 6.2°C and 8.9°C, respectively. With regard to the epoxy-0.2 CNT, addition of 0.2 wt.% NC resulted in a more considerable improvement of the HDT, while the concentration of the nanofiller was the same. NC layers effectively restrained the diffusion of small molecules in the crosslinked epoxy matrix, resulting in relatively higher dimensional stability of the composite.[40] Figure 8 shows that, at the loading of 0.2 wt.% CNC (epoxy-0.2 CNC), the HDT was increased by 9.7°C compared to the pristine polymer which caused the highest increase compared to the other nanofillers. As indicated before, the fraction of CNT within the CNC and PNC was about 50%. So, when the overall content of the hybrid filler was 0.2 wt.%, the actual loading level of CNT or NC was only about 0.1 wt.%. Although the increase in the HDT caused by the incorporation of 0.2 wt.% of the PNC was higher than epoxy-0.2 CNT, it was less than that of epoxy-0.2 NC. Thus, at the same content, the increasing effect of the physical hybrid on the HDT was less than NC alone. However, the enhancement in HDT upon incorporation of 0.2 wt.% of the CNC was even higher than that of epoxy nanocomposites using 0.2 wt.% CNT or 0.2 wt.% NC alone. The results clearly showed the benefit of using the CNC filler, due to its 3D structure as well as the strong interfacial interaction with the epoxy matrix shown previously by SEM.

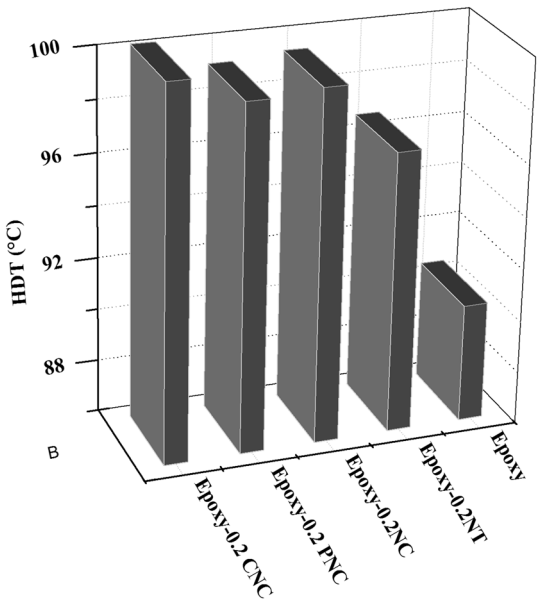

Fig. 8. Variation in HDT of epoxy nanocomposites with different nanofiller.

In order to shed further light on the effect of CNC on the thermal properties of the epoxy, the TGA/DTG of nanocomposites was considered (Fig. 9), from which it is revealed that the incorporation of the nanofiller enhanced the thermal stability of the epoxy. However, the extent of the improvement depends on the type of the nanofiller. The temperature of 5% weight loss and the temperature of the fastest decomposition rate are considered as the onset temperature of the decomposition (T_{on}) and degradation temperatures (T_{deg}), respectively. T_{on}, T_{deg} and residual mass for the nanocomposite samples are summarized in Table III. The degradation of the pristine epoxy started at 340°C, while the epoxy nanocomposite started to degrade at slightly higher temperatures. This can be the evidence of the improved thermal stability in the presence of nanofillers,[20] which acted as the barriers for heat loss and volatile degradation products in the nanocomposites.[14] The barrier behavior, called nano-confinement, has been reported to maximize when the nanofiller exerted an exfoliated morphology.[41] At the same concentration, the addition of NC resulted in a higher improvement of the thermal stability of the epoxy, compared to CNT. Similar behavior was reported for polyurethane by Ambuken et al.[42] The combination of the two fillers (both chemical and physical hybrids) produced further enhancements in thermal stability, which is in agreement with what has been observed for polyurethane foam and polyamide-6.[18,19] The increase in T_{on} and T_{deg} was more pronounced in the case of the chemical hybrid of CNT and NC (epoxy-0.2 CNC). Significant improvement in the thermal stability of the epoxy by the addition of the hybrid nanofillers can be attributed to the combined effect of the CNT and NC and their strong interfacial interactions with the polymer matrix. Synergistic effects of CNT and NC were more marked for the

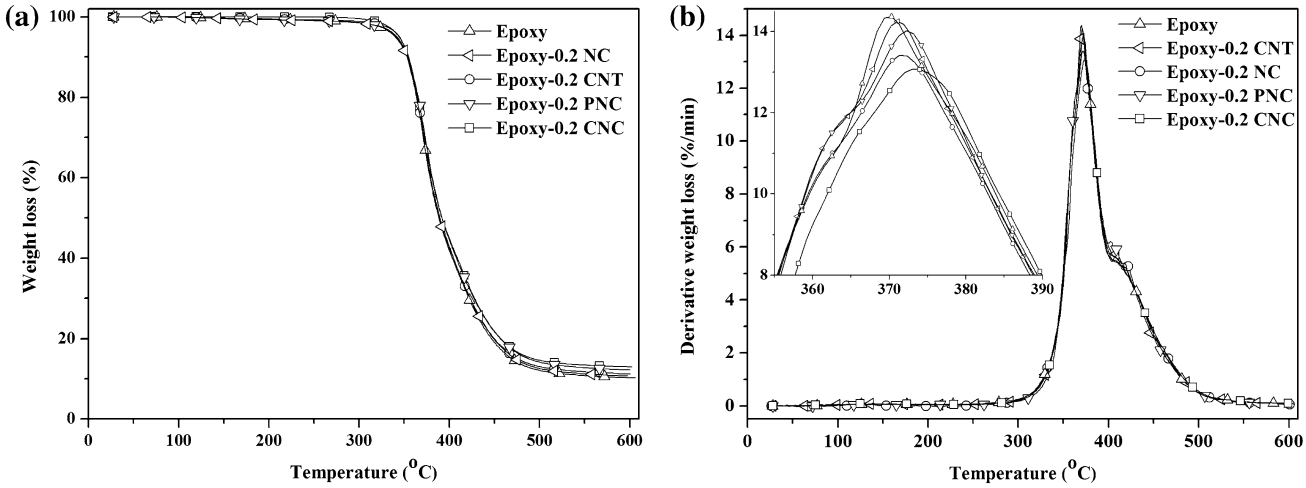

Fig. 9. (a) TGA and (b) DTG curves of epoxy nanocomposites with different nanofillers.

chemical hybrid compared to the physical one. It was believed that, in epoxy-0.2 CNC, the exfoliated state of NC in combination with the presence of CNT grown on their surfaces, resulted in the greater improvement of the thermal stability of the composites.[17] It was also noted that the presence of nanofiller was effective in improving the weight residues of the epoxy nanocomposites. The residual mass of the nanocomposites with different type of nanofiller was 1–2 wt.% higher than that of pure epoxy. This enhancement of the residual mass was ascribed to the high heat resistance caused by the presence of the nanofiller.[14]

Considering all thermal properties, although epoxy-0.2 CNC and epoxy-0.2 PNC have the same amount of CNT and NC, the increase in T_g, *HDT* and T_{deg} of epoxy is more remarked in epoxy-0.2 CNC. Therefore, this could be understood only as the result of the poor dispersion of PNC into the epoxy compared to CNC. This finding proved that NC and CNT have a more significant synergistic effect in improving the polymer thermal properties in the case of CNC.

CONCLUSION

The improving effect of the unique 3D CNT-NC hybrid nanofiller has been demonstrated in this study. The chemical hybrid of CNT and NC (CNC) was successfully fabricated through high-temperature decomposition of methane. The as-prepared CNC was added into an epoxy matrix in order to compare the properties of the obtained composite with nanocomposites prepared by CNT, NC and a physical mixture of these two (PNC).

Compared with the un-filled epoxy, T_{deg}, *HDT*, T_g and E' of the nanocomposite were greatly improved. Among all the nanofillers, the advantages and uniqueness of CNC as the filler for epoxy nanocomposites was more marked in its thermal properties. Synergistic effects of CNT and NC were obviously higher in the chemical hybrid compared to the physical one. The improvement was related to the 3D structure of the CNC observed from SEM and TEM. Furthermore, the growth of CNT on the NC surface in the CNC hybrid led to delamination of the NC in the epoxy matrix. This caused CNC to be more effective for improving the thermal performance of the epoxy. Such behavior justified the complexity of the process followed for the preparation of CNC hybrids.

REFERENCES

1. E. Esmizadeh, A. Yousefi, and G. Naderi, *Iran. Polym J.* 24, 1 (2015).
2. H. Dai, *Surf. Sci.* 500, 218 (2002).
3. Q.T. Nguyen and D.G. Baird, *Adv. Polym. Technol.* 25, 270 (2006).
4. D. Sun, C.C. Chu, and H.J. Sue, *Chem. Mater.* 22, 3773 (2010).
5. L. Liu and J.C. Grunlan, *Adv. Funct. Mater.* 17, 2343 (2007).
6. A.T. Mou'ad, S.H. Ahmad, A. Shamsul Bahri, and Y.L. Jiun, *Adv. Mater. Res.* 501, 194 (2012).
7. A.T. Mou'ad, S.H. Ahmad, K. Ahmad, K. Zarina, and H. Norita, *Adv. Mater. Res.* 576, 296 (2012).
8. T.D. Hapuarachchi, T. Peijs, and E. Bilotti, *Polym. Advan. Technol.* 24, 331 (2013).
9. P. Pandey, S. Mohanty, and S.K. Nayak, *High. Perform. Polym.* 26, 826 (2014).
10. S. Pack, T. Kashiwagi, D. Stemp, J. Koo, M. Si, J.C. Sokolov, and M.H. Rafailovich, *Macromolecules.* 42, 6698 (2009).
11. P. Pandey, S. Mohanty, and S.K. Nayak, *Chin. J. Chem. Eng.* 2014, 1 (2014).
12. A. Hazarika and T.K. Maji, *Chem. Eng. J.* 247, 33 (2014).
13. W. Zhang, I.Y. Phang, and T. Liu, *Adv. Mater.* 18, 73 (2006).
14. Y.Q. Zhao, K.T. Lau, Z. Wang, Z.C. Wang, H.Y. Cheung, Z. Yang, and H.L. Li, *Polym. Compos.* 30, 702 (2009).
15. M.Q. Zhao, Q. Zhang, X.L. Jia, J.Q. Huang, Y.H. Zhang, and F. Wei, *Adv. Funct. Mater.* 20, 677 (2010).
16. Z. Wang, C. Xu, Y. Zhao, D. Zhao, Z. Wang, H. Li, and K.-T. Lau, *Mater. Sci. Eng. A-Struct.* 490, 481 (2008).
17. A. Enotiadis, K. Litina, D. Gournis, S. Rangou, A. Avgeropoulos, P. Xidas, and K. Triantafyllidis, *J. Phys. Chem. B.* 117, 907 (2013).
18. L. Madaleno, R. Pyrz, A. Crosky, L.R. Jensen, J.C.M. Rauhe, V. Dolomanova, A.M.M.V. de Barros Timmons, J.J. Cruz Pinto, and J. Norman, *Compos. Part A* 44, 1 (2013).

19. C. Zhang, W.W. Tjiu, T. Liu, W.Y. Lui, I.Y. Phang, and W.D. Zhang, *J. Phys. Chem. B.* 115, 3392 (2011).
20. D. Manikandan, R.V. Mangalaraja, R.E. Avila, R. Siddheswaran, and S. Ananthakumar, *Mater. Sci. Eng. B Solid.* 177, 614 (2012).
21. E. Esmizadeh, A.A. Yousefi, G. Naderi, C. Milone, *Appl. Clay. Sci*. doi:10.1016/j.clay.2015.06.022.
22. N. Goulbourne, S. Son, and J. Fox, *The 14th International Symposium on: Smart Structures and Materials & Nondestructive Evaluation and Health Monitoring* (2007, International Society for Optics and Photonics).
23. C. Milone, M. Dhanagopal, S. Santangelo, M. Lanza, S. Galvagno, and G. Messina, *Ind. Eng. Chem. Res.* 49, 3242 (2010).
24. K. Wu, B.K. Kandola, E. Kandare, and Y. Hu, *Polym. Compos.* 32, 378 (2011).
25. E. Esmizadeh, G. Naderi, and M.H.R. Ghoreishy, *J. Appl. Polym. Sci.* 130, 3229 (2013).
26. P. Podsiadlo, B.S. Shim, and N.A. Kotov, *Coordin. Chem. Rev.* 253, 2835 (2009).
27. T. Tsoufis, L. Jankovic, D. Gournis, P.N. Trikalitis, and T. Bakas, *Mater. Sci. Eng. B Solid.* 152, 44 (2008).
28. A. Rinaldi, J. Zhang, J. Mizera, F. Girgsdies, N. Wang, S.B.A. Hamid, R. Schlögl, and D.S. Su. *Chem. Commun.* 6528 (2008).
29. J. Kim, M.K. Chung, H.K. Bok, J.H. Ku, S. Park, J. Ryu, and S.M. Oh, *J. Electrochem. Soc.* 157, A412 (2010).
30. M.S. Kim, G.H. Kim, and S.R. Chowdhury, *Polym. Eng. Sci.* 47, 308 (2007).
31. S. Santangelo, G. Gorrasi, R. Di Lieto, S. De Pasquale, G. Patimo, E. Piperopoulos, M. Lanza, G. Faggio, F. Mauriello, and G. Messina, *Appl. Clay Sci.* 53, 188 (2011).
32. A.K. Schaper, H. Hou, A. Greiner, and F. Phillipp, *J. Catal.* 222, 250 (2004).
33. L. Cancado, K. Takai, T. Enoki, M. Endo, Y. Kim, H. Mizusaki, A. Jorio, L. Coelho, R. Magalhaes-Paniago, and M. Pimenta, *Appl. Phys. Lett.* 88, 163106 (2006).
34. L. Jankovic, D. Gournis, K. Dimos, M. Karakassides, and T. Bakas *Journal of Physics Conference Series* (IOP Publishing, 2005).
35. A.D. Purceno, B.R. Barrioni, A. Dias, G.M. da Costa, R.M. Lago, and F.C. Moura, *Appl. Clay Sci.* 54, 15 (2011).
36. L. Madaleno, R. Pyrz, L.R. Jensen, J.J. Pinto, A.B. Lopes, V. Dolomanova, J. Schjødt-Thomsen, and J.C.M. Rauhe, *Compos. Sci. Technol.* 72, 377 (2012).
37. Q. Li, H. Yan, J. Zhang, and Z. Liu, *Carbon* 42, 829 (2004).
38. A. Hajibaba, G. Naderi, E. Esmizadeh, and M.H.R. Ghoreishy, *J. Compos. Mater.* 48, 131 (2012).
39. R. Arora, N. Singh, K. Balasubramanian, and P. Alegaonkar, *RSC. Adv.* 4, 50614 (2014).
40. G. Khanbabaei, J. Aalaie, A. Rahmatpour, A. Khoshniyat, and M. Gharabadian, *J. Macromol. Sci. Phys.* 46, 975 (2007).
41. M.C. Costache, M.J. Heidecker, E. Manias, G. Camino, A. Frache, G. Beyer, R.K. Gupta, and C.A. Wilkie, *Polymer* 48, 6532 (2007).
42. P.V. Ambuken, H.A. Stretz, J.H. Koo, J.M. Messman, and D. Wong, *Polym. Degrad. Stabil.* 102, 160 (2014).